The ATCA 13-cm Polarimetric Response

R.J. Sault M. Ehle

14 May 1996

Summary: The 13-cm ATCA off-axis polarimetric response is characterised and simulated. Spurious polarimetric features of greater than 10% can result in features somewhat beyond the half power radius. A technique to correct for these errors is presented. This appears to reduce the error by a factor of 3 to 8. For strong point sources, the limit to the technique appears to be the quality of the model of the instrumental polarisation. For more complex objects, normal calibration and deconvolution errors may limit the technique.

1 Introduction

Because of an error in the feed-horn fin design, 13-cm observations with the ATCA suffer significant off-axis instrumental polarisation. It is at least a factor of 3 to 5 times worse than the other ATCA bands. This memo describes the measurement, modelling and simulation of the polarimetric response of the 13-cm system.

As an example, Fig. 1 gives images from an 11-hour observation offset by 420 arc seconds from 1934-638. A 1.5-km array was used (antenna 6 was excluded in the imaging). The apparent flux density is 8.51 Jy (primary beam attenuation has reduced this from the true value of 11.58 Jy), and the source has apparent peak values of Q, U and V of 1.8%, 0.6% and 0.8% (in reality the source is unpolarised). If the offset was at the half-power point (630 arc seconds), the off-axis error would be approximately a factor of 4 worse than in this observation.

2 Measurement and Reduction

To measure the polarimetric response, we observed 1934-638 over a period of 8 hours. By scanning it through the primary beam, we were able to determine the polarimetric response of the primary beam.

During the observation time, we scanned phase/pointing centre by ±40 arc min in RA, and then ±40 arc min in DEC, with the scans always centred on 1934-638. We integrated at 2 arc min steps along each scan. With this scanning pattern, we observed 1934-638 'on-source' about every 10 minutes. Because of parallactic rotation, when considered in the frame of the primary beam, these scans rotated by about 130° during the course of the observation. So the sampling that we achieved is a cross rotated through 130°. Thus we have good coverage of the primary beam, and sampled 45% of it twice (once with RA scans, the other time with DEC scans). When we did sample the same part of the primary beam twice, we obtained consistent results, reassuring us that there are no significant time or elevation effects.

Fairly normal techniques were used for the initial reduction of the data. The data were flagged and then calibrated. The 'on-source' measurements of 1934-638 were used as the bandpass/primary/secondary/polarimetric calibrator. Calibration solutions were then applied to all the data (polarimetrically, we corrected the response at the pointing centre). During the course of the observation, the phase centre was allowed to follow the pointing centre. So after calibration, we applied a phase shift to the data to re-phase it back to the position of 1934-638. We then phase self-calibrated, using a solution interval of 1 integration (10 seconds), and using data where there was still at least 1 Jy of signal.

During the reduction, we did not perform any spectral averaging. This was essential as the phase slope across the band was significant when collection data at a significant distance from 1934-638. Re-phasing to the position of 1934-638 eliminated this slope. However there was still a noticeable de-correlation caused by bandwidth smearing within one channel. Naturally this affects mainly the longest baselines. In the final fitting process, we used data from only the two shortest baselines (both about 500 m).

3 Characterisation

Here we note qualitatively some characteristics of the 13-cm polarimetric response.

- All baselines show a very similar response, and the XY and YX correlations are conjugates of each other. This implies that all the antennas have the same polarimetric response, which is not unexpected.
- One normally expects that if one takes a slice through a primary beam, that this slice will show a symmetric function. This is not the case for the 13-cm system. Both in terms of its total intensity primary beam and its instrumental polarisation, the response is skewed. The skewness of the total intensity response was first noted by Derek McKay, who noted that his pointing solutions were different for the XX and YY correlations.

  Expressing it in another way, consider describing the response at a particular radius from the pointing centre as a function of the position angle of that point. For a symmetric response this will be describable in terms of cos and sin functions of 2ψ and higher even harmonics. For a skewed response, there will be components with odd harmonics as well. For the 13-cm system, the XY and YX response is almost purely $\cos\psi$ and $\sin\psi$ components. Although the dominant component in the XX and YY is a 2ψ one, there are significant ψ components.
- If the X and Y feeds were identical apart from a 90° rotation, we would expect that the XX and YY data would be the same apart from a 90° shift around the primary beam. Although this is true to a moderate extent, the data does show that this is not entirely the case. For example, in Fig. 2, the intensity of the two minima in the XX and YY plots cannot be explained by the X and Y feeds simply being 90° rotated versions of each other.

A plot of instrumental polarisation as a function of distance from the pointing centre is given in Figure 3 (this plot shows good agreement to a preliminary one produced some months ago). Note this gives the ratio of the apparent polarised emission to the *true* total intensity, not the *apparent* total intensity. To get, for example, the

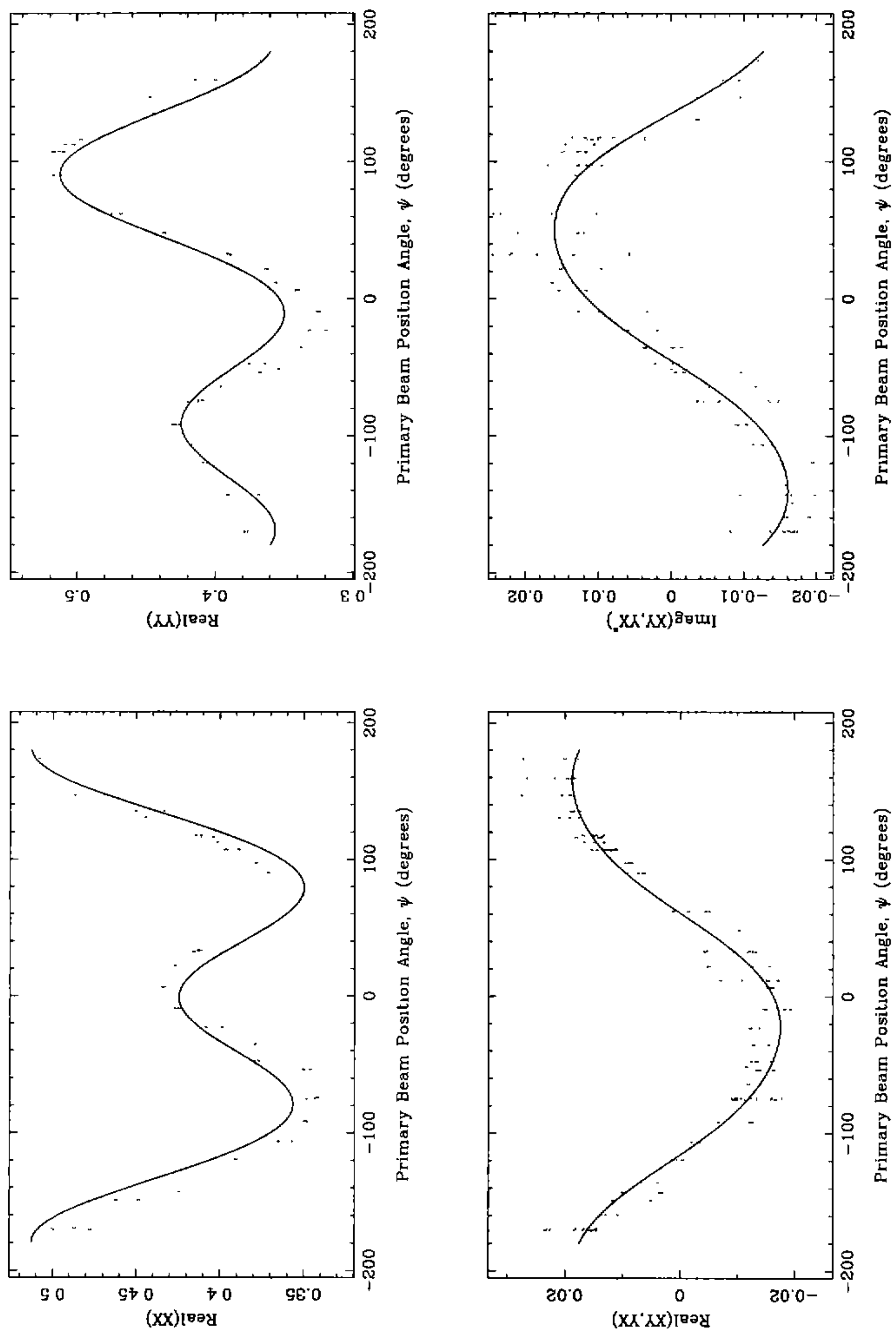

Figure 2: Data and fitted curves. The data are plotted as a function of primary beam position angle, ψ, and represent the response at distance of 12 arc min from the pointing centre. The fits represent the form discussed in Sect. 4.

Fairly normal techniques were used for the initial reduction of the data. The data were flagged and then calibrated. The 'on-source' measurements of 1934-638 were used as the bandpass/primary/secondary/polarimetric calibrator. Calibration solutions were then applied to all the data (polarimetrically, we corrected the response at the pointing centre). During the course of the observation, the phase centre was allowed to follow the pointing centre. So after calibration, we applied a phase shift to the data to re-phase it back to the position of 1934-638. We then phase self-calibrated, using a solution interval of 1 integration (10 seconds), and using data where there was still at least 1 Jy of signal.

During the reduction, we did not perform any spectral averaging. This was essential as the phase slope across the band was significant when collection data at a significant distance from 1934-638. Re-phasing to the position of 1934-638 eliminated this slope. However there was still a noticeable de-correlation caused by bandwidth smearing within one channel. Naturally this affects mainly the longest baselines. In the final fitting process, we used data from only the two shortest baselines (both about 500 m).

3 Characterisation

Here we note qualitatively some characteristics of the 13-cm polarimetric response.

- All baselines show a very similar response, and the XY and YX correlations are conjugates of each other. This implies that all the antennas have the same polarimetric response, which is not unexpected.
- One normally expects that if one takes a slice through a primary beam, that this slice will show a symmetric function. This is not the case for the 13-cm system. Both in terms of its total intensity primary beam and its instrumental polarisation, the response is skewed. The skewness of the total intensity response was first noted by Derek McKay, who noted that his pointing solutions were different for the XX and YY correlations.

  Expressing it in another way, consider describing the response at a particular radius from the pointing centre as a function of the position angle of that point. For a symmetric response this will be describable in terms of cos and sin functions of 2ψ and higher even harmonics. For a skewed response, there will be components with odd harmonics as well. For the 13-cm system, the XY and YX response is almost purely $\cos\psi$ and $\sin\psi$ components. Although the dominant component in the XX and YY is a 2ψ one, there are significant ψ components.
- If the X and Y feeds were identical apart from a 90° rotation, we would expect that the XX and YY data would be the same apart from a 90° shift around the primary beam. Although this is true to a moderate extent, the data does show that this is not entirely the case. For example, in Fig. 2, the intensity of the two minima in the XX and YY plots cannot be explained by the X and Y feeds simply being 90° rotated versions of each other.

A plot of instrumental polarisation as a function of distance from the pointing centre is given in Figure 3 (this plot shows good agreement to a preliminary one produced some months ago). Note this gives the ratio of the apparent polarised emission to the *true* total intensity, not the *apparent* total intensity. To get, for example, the

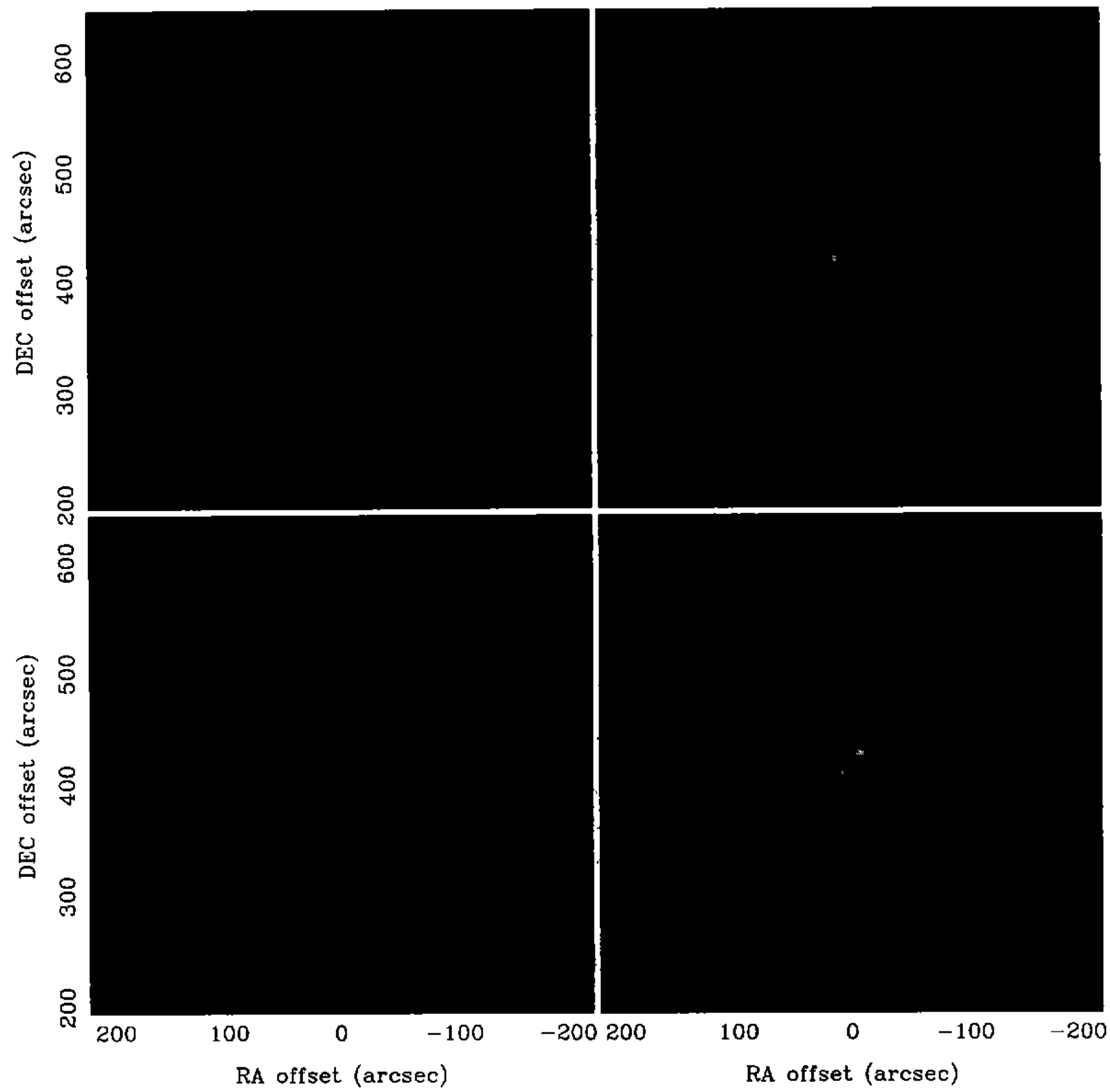

Figure 1: Off-axis polarimetric response to 1934-638 offset by 420 arc seconds. The images are I (top left), Q (top right), U (bottom left) and V (bottom right). The intensity range represented is ± 0.1 Jy.

AT/ 39.3/088

The ATCA 13-cm Polarimetric Response

R.J. Sault M. Ehle

14 May 1996

Summary: The 13-cm ATCA off-axis polarimetric response is characterised and simulated. Spurious polarimetric features of greater than 10% can result in features somewhat beyond the half power radius. A technique to correct for these errors is presented. This appears to reduce the error by a factor of 3 to 8. For strong point sources, the limit to the technique appears to be the quality of the model of the instrumental polarisation. For more complex objects, normal calibration and deconvolution errors may limit the technique.

1 Introduction

Because of an error in the feed-horn fin design, 13-cm observations with the ATCA suffer significant off-axis instrumental polarisation. It is at least a factor of 3 to 5 times worse than the other ATCA bands. This memo describes the measurement, modelling and simulation of the polarimetric response of the 13-cm system.

As an example, Fig. 1 gives images from an 11-hour observation offset by 420 arc seconds from 1934-638. A 1.5-km array was used (antenna 6 was excluded in the imaging). The apparent flux density is 8.51 Jy (primary beam attenuation has reduced this from the true value of 11.58 Jy), and the source has apparent peak values of Q, U and V of 1.8%, 0.6% and 0.8% (in reality the source is unpolarised). If the offset was at the half-power point (630 arc seconds), the off-axis error would be approximately a factor of 4 worse than in this observation.

2 Measurement and Reduction

To measure the polarimetric response, we observed 1934-638 over a period of 8 hours. By scanning it through the primary beam, we were able to determine the polarimetric response of the primary beam.

During the observation time, we scanned phase/pointing centre by ±40 arc min in RA, and then ±40 arc min in DEC, with the scans always centred on 1934-638. We integrated at 2 arc min steps along each scan. With this scanning pattern, we observed 1934-638 'on-source' about every 10 minutes. Because of parallactic rotation, when considered in the frame of the primary beam, these scans rotated by about 130° during the course of the observation. So the sampling that we achieved is a cross rotated through 130°. Thus we have good coverage of the primary beam, and sampled 45% of it twice (once with RA scans, the other time with DEC scans). When we did sample the same part of the primary beam twice, we obtained consistent results, reassuring us that there are no significant time or elevation effects.

ratio of *apparent* polarised emission to *apparent* total intensity at the half-power point, we would double the number on the plot, giving a worst-case value of about 9% linear polarisation and 2% circular.

4 Modelling

The simplest approach to modelling the instrumental polarisation is to derive Jones matrices which describe the response (a Jones matrix is simply a 2×2 'voltage' matrix which describes the linear process by which two nominally orthogonal polarised signals are transmitted through a system – see Hamaker, Bregman & Sault 1996). Because the polarimetric response varies across the primary beam, so too will the Jones matrix (i.e. each point in the primary beam is described by a potentially different Jones matrix). Given a Jones matrix, J, the coherence matrix is simply given by

$$\begin{pmatrix} XX & XY \\ YX & YY \end{pmatrix} = JJ^{\mathbf{T}*} \tag{1}$$

As noted earlier, the responses of the different antennas are largely the same, and so a single family of Jones matrices common to all antennas will suffice. Additionally we will assume that the X and Y probes have the same response (apart from a rotation of 90°). There is evidence that this is not so. However the differences in response between the X and Y probes are a small fraction of the off-axis response, and so can be ignored for our purposes. Given these assumptions, the Jones matrix of an antenna will be of the general form:

$$J = \begin{pmatrix} A(r,\psi) & B(r,\psi) \\ -B(r,\psi-\frac{3}{2}\pi) & A(r,\psi-\frac{3}{2}\pi) \end{pmatrix}. \tag{2}$$

Here r is the distance from the pointing centre and we define ψ as the angle from the axis of the X probe to a point in the primary beam (all angles here are measured in the direction celestial north towards east). The lower row of the Jones matrix represents the response of the Y feed. The sign change of B and the angle of $3\pi/2$ is needed to account for the Y feed being rotated by 90° relative to the X.

The fact that the angle is $3\pi/2$ rather than $\pi/2$ requires explanation. It is because here we assume that, apart from a 90° rotation, the on-line system feed A is polarimetrically equivalent to feed B. These feeds are at +45° and −45° to the elevation axis respectively. Whereas A corresponds to Miriad's X feed, the negative of B corresponds to the Y feed. This is because Miriad follows the normal convention that the Y feed is at +90° to the X (and fiddles the data in `atlod` to make it so).

Because our experiment used an unpolarised calibrator as a probe of the polarimetric response, there are some aspects of the polarimetric response that our experiment is fundamentally insensitive to (Sault, Hamaker & Bregman 1996). For most sources this is unimportant, as the main cause of problems in astronomical interpretation results from the strong total intensity leaking into the weaker polarised emission.

Empirically, we find that we can fit $A(r,\psi)$ and $B(r,\psi)$ by

$$A(r,\psi) = a_1 + a_2\cos(2\psi) + a_3\cos\psi + a_4\sin\psi, \tag{3}$$
$$B(r,\psi) = (a_5 + ia_6)\sin\psi + a_7\cos\psi. \tag{4}$$

Here the a coefficients (which are real-valued) are all functions of r. The term a_1 corresponds to the normal 'voltage primary beam' response. All the other terms are unwanted error terms.

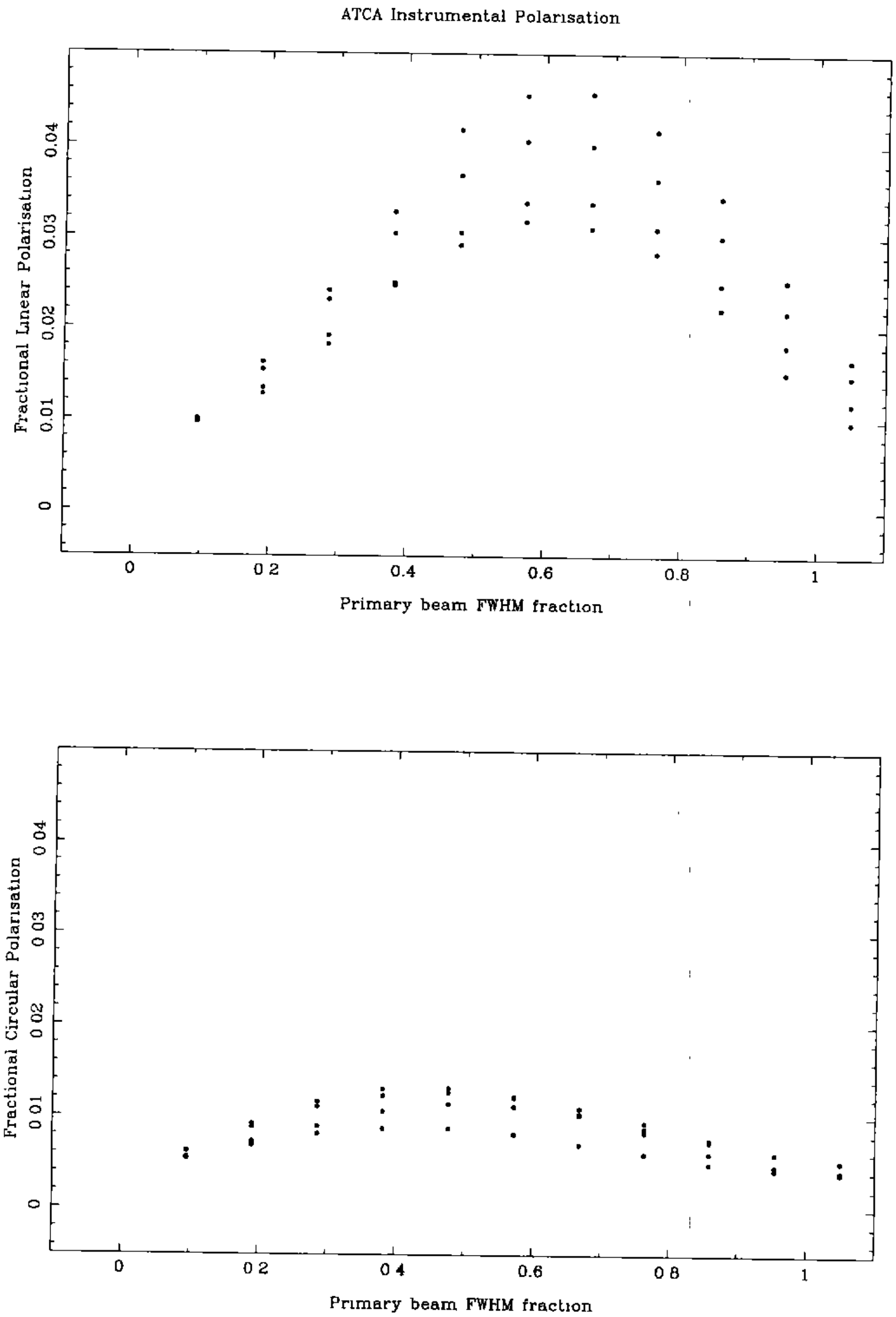

Figure 3: Instrumental polarisation at 13 cm as a function of radius. This gives the *apparent* polarised emission as a fraction of the *true* total intensity.

For comparison, the theoretical form of $A(r,\psi)$ and $B(r,\psi)$ for an ideal paraboloid (Ghobrial 1976) is

$$A(r,\psi) = a_1 + a_2\cos(2\psi) \quad (5)$$
$$B(r,\psi) = a_2\sin(2\psi) \quad (6)$$

We know the 6-cm system follows this form reasonably closely, with a_1 being (roughly) the voltage primary beam pattern and a_2 being somewhat less than 1% at the half-power point.

In modelling the 13-cm response, we assume a_1 follows a Gaussian form and fit for the voltage primary beam FWHM. The largest error term corresponds to a_2, which is about 4% at the primary beam half-power point. We fit this using the form $\alpha\sin^2(r/r_0)$. The other terms are 2% or less at the half-power point, and are fitted with the form $\alpha r + \beta r^2$. Figure 4 gives the value of the a coefficients as a function of r. Figure 2 gives some data as a function of ψ along with the fit.

5 Simulations

The polarimetric response model described above was included within a special version of Miriad's **uvgen** task (a task to produce fake observations). Using this, we simulated an observation similar to the one that we actually did, and generated a simulated version of Fig. 3. The fact that the plots were very similar reassures us that the model we are using is a reasonable one, and that the simulation software works.

Next we simulated a 12-hour observation of an unpolarised spiral-like object. The simulation was for the 375-m array, and excluded antenna 6 in the imaging step. Figures 5, 6 and 7 give the apparent total intensity, fractional linear polarisation (including position angle vectors) and fractional circular polarisation, respectively. All are deconvolved images. The fact that the polarised emission is spurious is not that apparent in the deconvolved images (i.e. instrumental problems are not obvious to the casual eye). The primary beam half-power point is drawn on these figures as a large circle. The instrumental effects do not produce significant errors in the total intensity image. However spurious fractional linear and circular polarisations of 13% and 5% are seen in these figures, both occurring in the eastern-most feature (i.e. the feature furtherest from the pointing centre). Clearly significant care is needed in interpreting large-field images of polarised emission at 13-cm.

6 Correction

Given that we can simulate the polarimetric response, then it is clear that we can, at least partially, correct for it. As the total intensity usually dominates, to good approximation we can ignore the corrupting influences of the polarised emission. Thus given a model of the total intensity, we can compute the error that would be expected in XX, YY, XY and YX, and subtract this off. A Miriad task (task **offaxis**) has been written to perform this operation.

As the simulation and correction software both use the same model of the off-axis polarimetric response (which only approximates the true off-axis response), simulation is not an appropriate tool to determine the effectiveness of the correction scheme. Nor is an appropriate, testing, observation readily available. Instead we

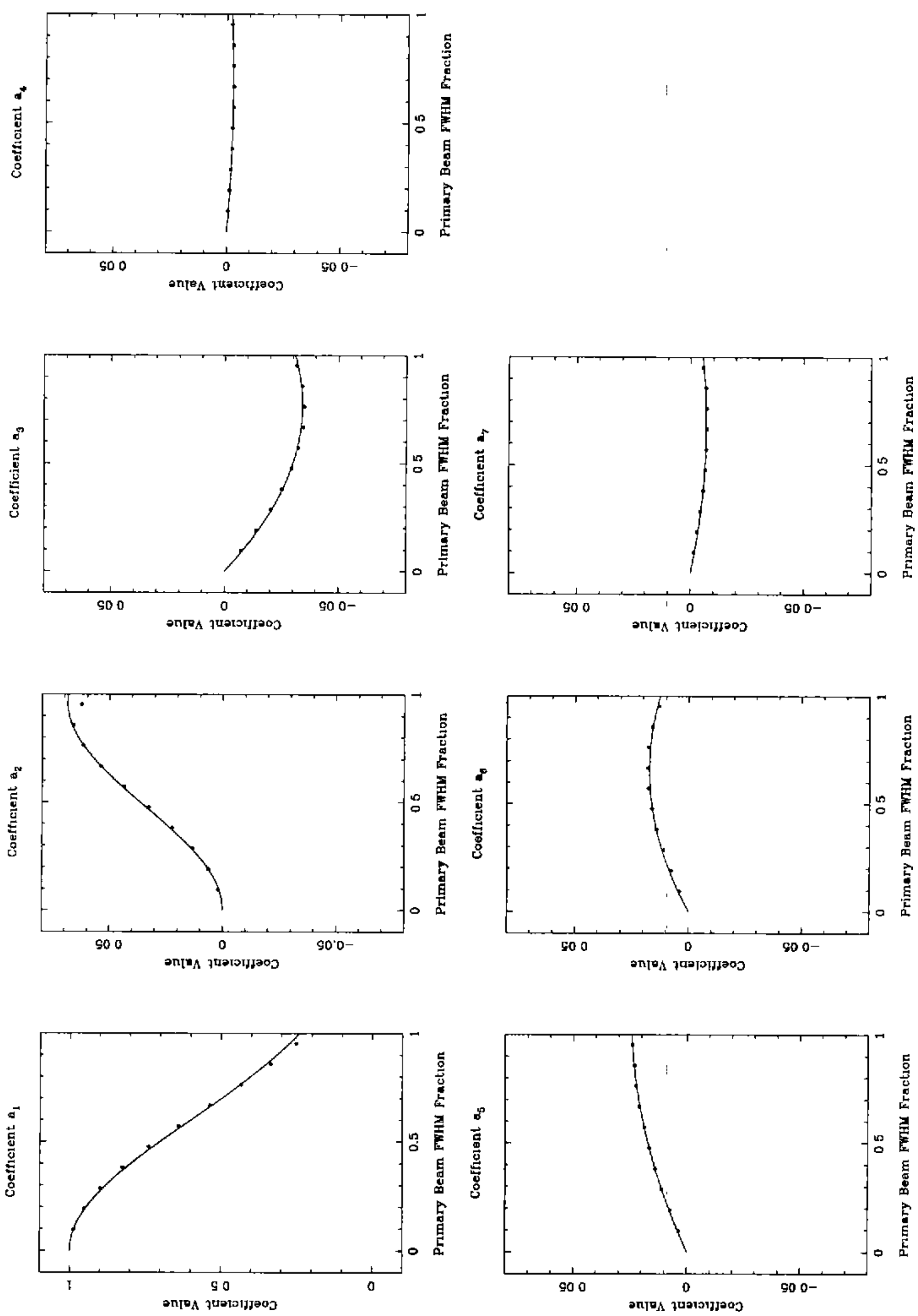

Figure 4: Coefficients of the Jones matrix as a function of radius.

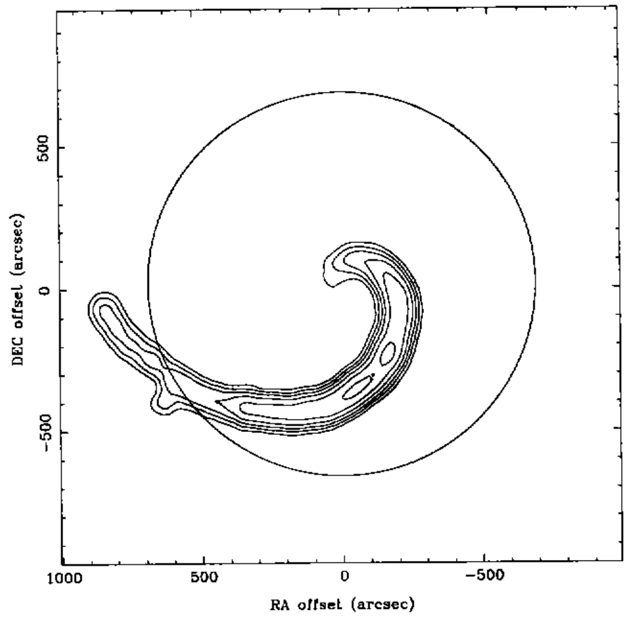

Figure 5: Apparent total intensity of the spiral object. Contours are drawn at 2%, 5%, 10%, 20%, 40% and 80%.

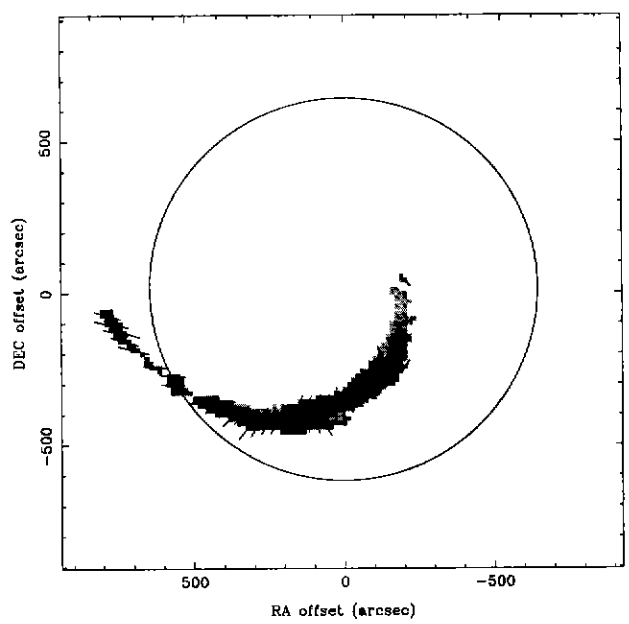

Figure 6: Apparent fractional linear polarisation of the spiral object. The intensity range is ±10%. The largest apparent linear polarisation is 13%, and is present in the eastern-most feature. The vectors denote the position angle of the linearly polarised emission.

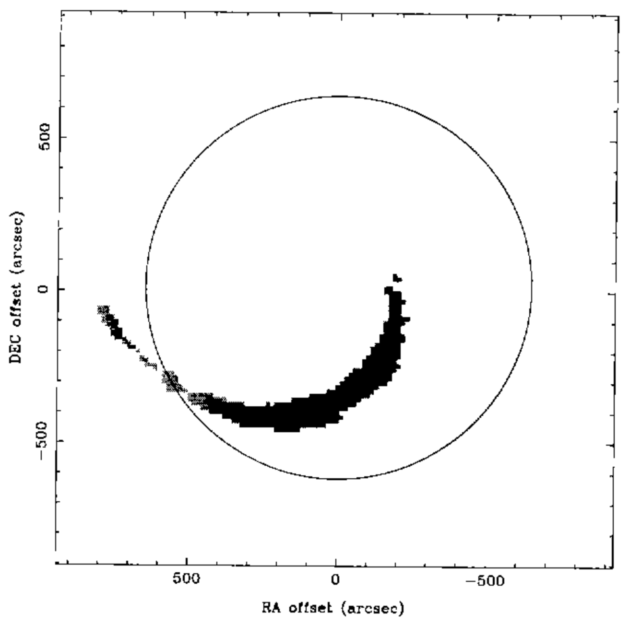

Figure 7: Apparent fractional circular polarisation of the spiral object. The intensity range is ±10%. The largest apparent circular polarisation is 5% and is present in the eastern-most feature.

show the correction scheme applied to the data presented in Fig. 1. Figure 8 gives the images which result after correction, with the apparent Q, U and V having changed to 0.6%, 0.6% and 0.1% respectively. Whereas Q and V have improved by factors of 3 and 8 respectively, U has remained essentially unchanged (although the error pattern has changed).

It is probably an artifact of the particular parallactic angle coverage that instrumental Q has been reduced but U has not. The greater improvement in V (compared with Q and U) reflects that our model of the diagonal elements of the Jones matrix is poorer than the off-diagonal ones. Instrumental gain errors do not appear to be the problem (the residual error patterns appear too ordered for this). Quite possibly better modelling of the diagonal Jones matrix errors will improve the correction in this experiment.

This test represents a best-case example: we have a simple point source, the data was (phase) self-calibrated, and there was no problem with bandwidth smearing with the 1.5-km array used. Thus this represents the best improvement that we can expect. For a more complex object, the correction will be less successful and will require a significant amount of computing.

References

Ghorbrial S.I., 1976, IEEE Trans. Antenna Propagation, AP-24, 418

Hamaker J.P., Bregman J.D., Sault R.J., 1996, to appear in A&AS

Sault R.J., Hamaker J.P., Bregman J.D., 1996, to appear in A&AS

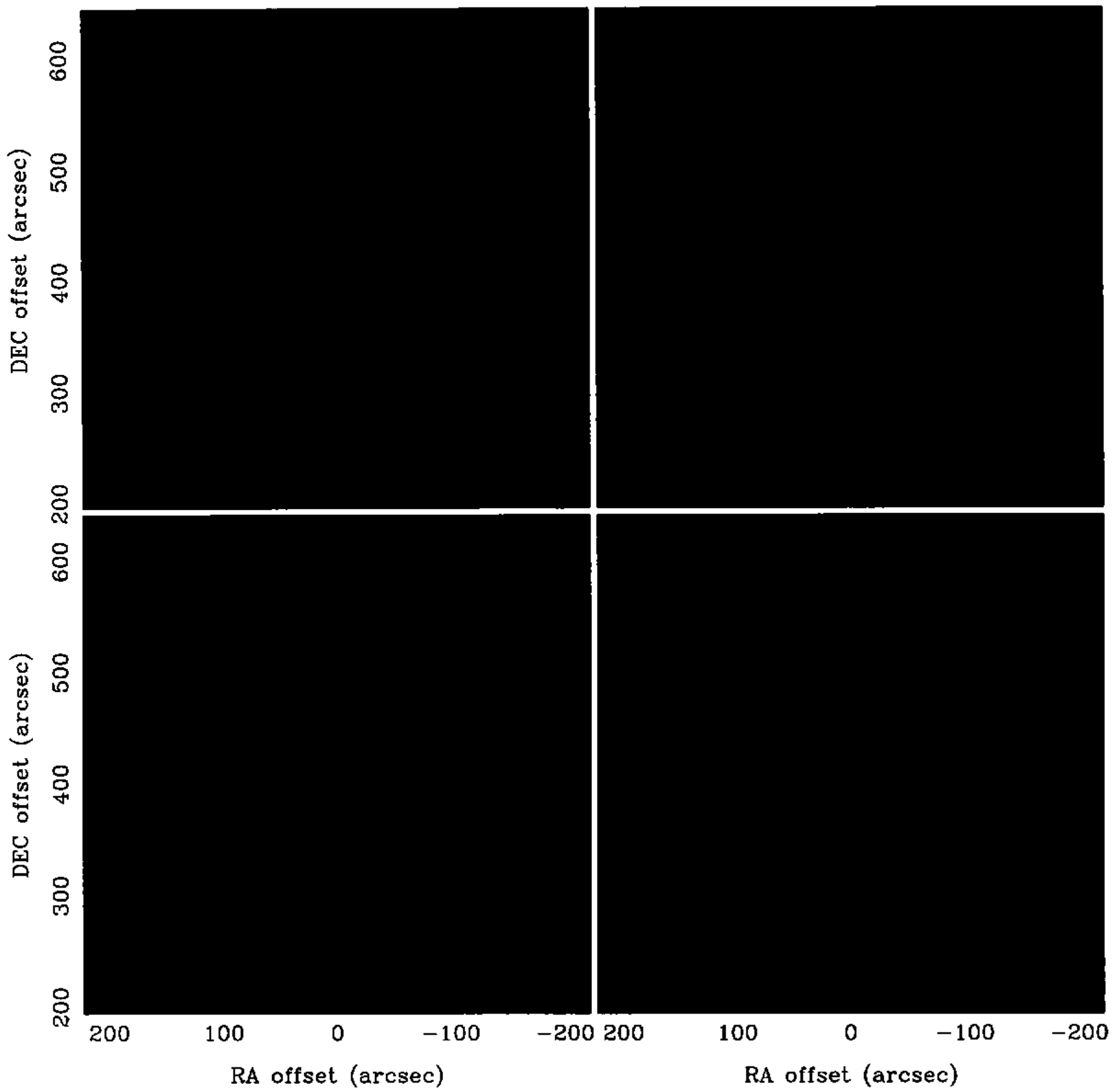

Figure 8: Off-axis polarimetric response to 1934-638 after correction. This should be compared with Fig. 1. The intensity range represented is ±0.1 Jy.